Supporting information for:

Butyl rubber-based interpenetrating polymer networks with side chain crystallinity: Self-healing and shape-memory polymers with tunable thermal and mechanical properties

Esra Su [a], Gozde Bayazit [b], Semra Ide [b], Oguz Okay [a, *]

a *Department of Chemistry, Istanbul Technical University, 34469 Maslak, Istanbul, Turkey*
b *Department of Physics Engineering and Department of Nanotechnology and Nanomedicine, Hacettepe University, 06800 Beytepe, Ankara, Turkey*

Table of contents:

SAXS analysis

SAXS data were collected at 23 °C with an exposure time of 900 s using the HECUS-SWAXS system (Graz, Austria). Nickel-filtered Cu Kα radiation ($\lambda = 0.154$ nm) operating at 50 kV/40 mA was used as the X-ray source. Guinier analyses, structural modeling, pair distance distribution calculations and 3D ab-initio shape (morphology) determinations were carried out to reach SAXS analyses' quantitative results with the help of IGOR Pro6 and DAMMIN programs [S1-S3]. Moore's Indirect Fourier Transformation (IFT) method was used for morphology determinations by using the scattering data which measured in the q range of 0.002-0.05 Å^{-1} [S4].

Cross-link density of IPNs

The effective cross-link density v_e of IPNs can be expressed by,

$$v_e = v_{e,cry} + v_{e,assoc} + v_{e,chem} \tag{S1}$$

where $v_{e,cry}$, $v_{e,assoc}$, and $v_{e,chem}$ are the components of the cross-link density v_e due to the lamellar crystals, associations between C18 side chains, and covalent cross-links, respectively. Because all these cross-links are effective at temperatures below T_m, the total effective cross-link density v_e can be estimated from the value of G' measured at 25 °C using the equation [S5-S7],

$$v_e = \frac{G'_{25°C}}{R\,T\,\phi_2^o} \tag{S2}$$

where R and T are in their usual meanings, and ϕ_2^o is the volume fraction of cross-linked polymer in as-prepared IPN. Moreover, above T_m, IPNs are in amorphous state so that the $v_{e,assoc}$, and $v_{e,chem}$ still existing in this state is related to G' measured at 65 °C by

$$v_{e,assoc} + v_{e,chem} = \frac{G'_{65°C}}{R\,T\,\phi_2^o} \tag{S3}$$

In a good solvent such as toluene, hydrophobic associations and lamellar crystals disappear while the 3D network structure can only be preserved by chemical cross-links [S8-S11]. Hence, $v_{e,chem}$ can be estimated from the Flory-Rehner equation [S6],

$$v_{e,chem} = \frac{-[ln(1-\phi_2) + \phi_2 + \chi (\phi_2)^2]}{V_1 \left[\phi_2^{1/3} (\phi_2^o)^{2/3} - \phi_2/2\right]} \tag{S4}$$

where ϕ_2 is the IPN volume fraction in equilibrium swollen state in toluene, χ is the polymer-solvent interaction parameter, and V_1 is the molar volume of toluene.

For calculations, we assume affine deformation of the IPN network, and G' at the frequency of 6.32 rad·s^{-1} is equal to the shear modulus G. Moreover, the following values were used in the calculations: $\chi = 0.49 + 0.25 \phi_2$ for IIR-toluene system [S12], $V_1 = 106$ mL·mol^{-1}, $\phi_2 = (1 - w_{sol}) d_1/(\rho q_w)$ where ρ are d_1 are the densities of IIR (0.92 g·mL^{-1}), and toluene (0.867 g·mL^{-1}), respectively, $v_2^o = 0.73 (1 - w_{sol})$. Table S3 and Fig. S6 show the swelling degree q_w and the soluble fraction w_{sol} of IPNs used in the calculations while the cross-link density components of IPNs calculated using Eqs. S1-S4 are compiled in Fig. S7.

Theoretical versus effective chemical cross-link density ($v_{e,chem}$) of IPNs

Butyl rubber (IIR) used in the IPN preparation has an unsaturation degree of 1.7 ± 0.2 mol %, that is, it consists of 1.7 ± 0.2 mol % isoprene units, the rest being isobutylene units with molecular weights M_r of 68 and 56 g/mol, respectively. This means that 1 g of IIR contains 0.30 ± 0.8 mmol isoprene units. Assuming that each unsaturation in IIR produces 4 elastically effective cross-links, the theoretical chemical cross-link density $v_{e,chem,theo}$, i.e., the number of network chains per volume, will be 111 ± 13, 167 ± 19, and 222 ± 27 mol ·m^{-3}, for IPNs with 20, 30, and 40 wt% IIR, respectively. These values are 3-orders of magnitude smaller as compared to the effective chemical cross-link densities $v_{e,chem}$ listed in Table S4.

Table S1. G' of IPN's in as-prepared state in toluene at 30 °C, and after removing toluene at 25 and 65 °C. $\omega = 6.28$ rad·s^{-1}.

IIR wt%	G' / kPa		
	as-prepared state at 30 °C	toluene-free at 25 °C	toluene-free at 65 °C
20	3.7	13x10^3	16
40	9	1.6x10^3	28
60	20	3.3x10^2	67
80	26	2.3x10^2	83

Table S2. Thermal and mechanical properties of IPN's. The explanations are given in the text.

IIR wt%	T_m / °C	T_{cry} / °C	f_{cry} %	E / MPa	W / MPa	ε_f %
20	50 (1)	40 (1)	25 (1)	35 (3)	2.3 (0.1)	82 (3)
30	50 (1)	39 (1)	25 (2)	16 (2)	5.5 (0.4)	257 (27)
40	51 (1)	42 (1)	14.6 (0.2)	3.9 (0.3)	11 (1)	656 (21)
50	50 (1)	41 (1)	9.5 (0.1)	2.2 (0.1)	11 (1)	827 (44)
60	48 (1)	41 (1)	6.7 (0.1)	1.2 (0.1)	12 (1)	1135 (60)
70	47 (1)	40 (2)	3.6 (0.2)	1.0 (0.1)	7.7 (0.7)	1156 (108)
80	46 (1)	40 (1)	1.5 (0.4)	0.68 (0.07)	5.3 (0.5)	1178 (103)

Table S3. The equilibrium weight swelling ratio q_w in toluene, and soluble fraction w_{sol} of IPNs at various IIR wt%.

IIR wt%	q_w	w_{sol} %
20	49 (3)	35 (1)
30	42 (3)	33 (1)
40	44 (1)	40 (2)
50	40 (1)	65 (6)
60	38 (1)	68 (5)
70	38 (1)	69 (4)
80	25 (2)	53 (3)

Table S4. $\nu_{e,cry}$, $\nu_{e,assoc}$, and $\nu_{e,chem}$ calculated using eqs S1-S4 for IPNs with various IIR contents.

IIR wt%	$\nu_{e,chem}$	$\nu_{e,cry}$	$\nu_{e,assoc}$	Crys %	Assoc %	Chem %
20	0.121	11629	12	99.9	0.1	0.001
40	0.134	1415	30	97.9	2.1	0.009
60	0.088	475	95	83.3	16.6	0.015
80	0.288	216	100	68.2	31.7	0.091
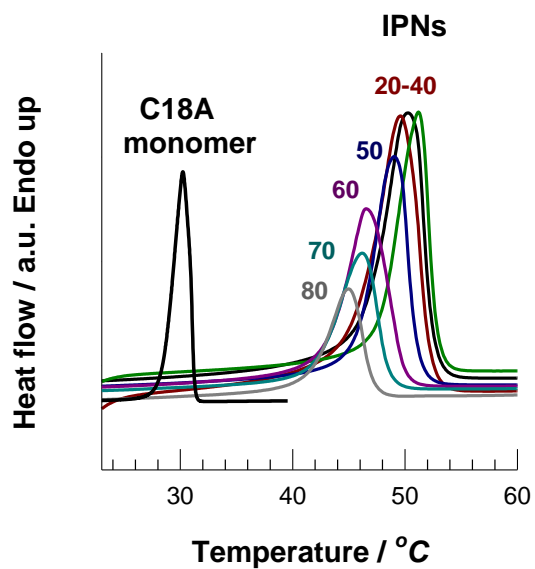
Fig. S1. DSC scans of C18A monomer, and IPNs at various IIR wt% as indicated.
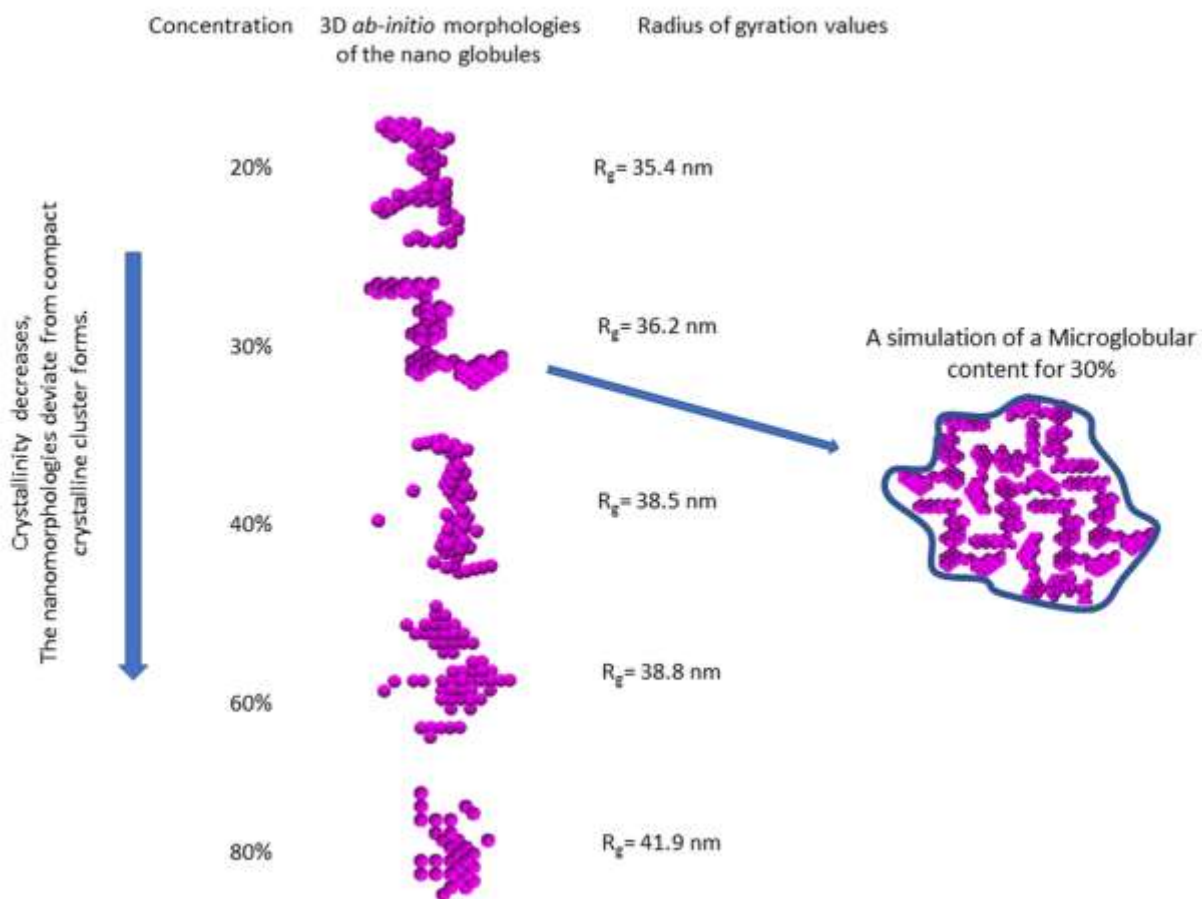
Fig. S2. The size and shape information of nanoglobules.
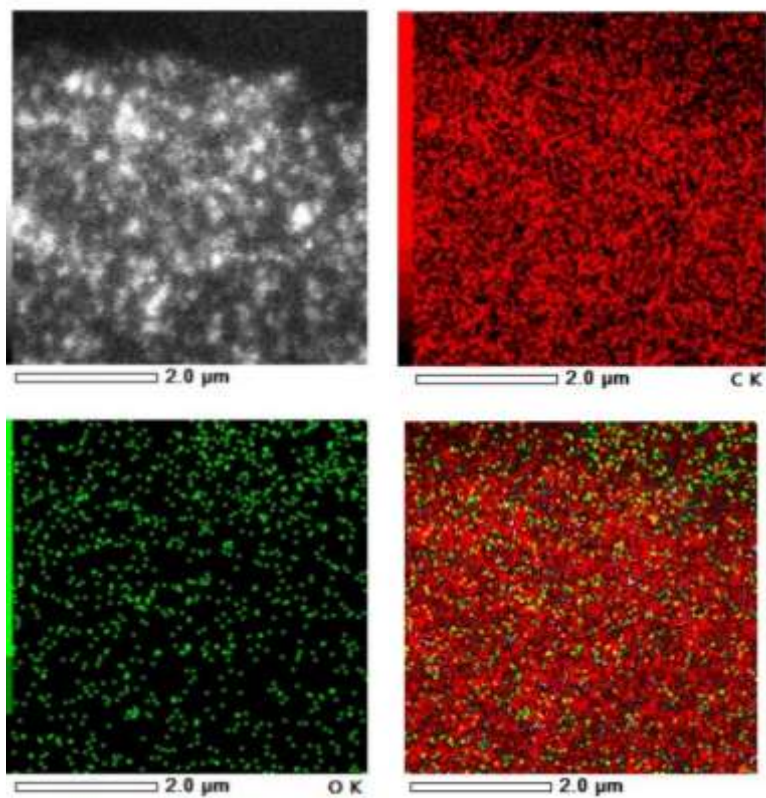
Fig. S3. STEM image and EDX maps of the IPN with 80 wt% IIR. Scale bars: 2 μm. The EDX maps show carbon (C) and oxygen (O) atoms in red and green, respectively, while their overlapping areas appear yellow.
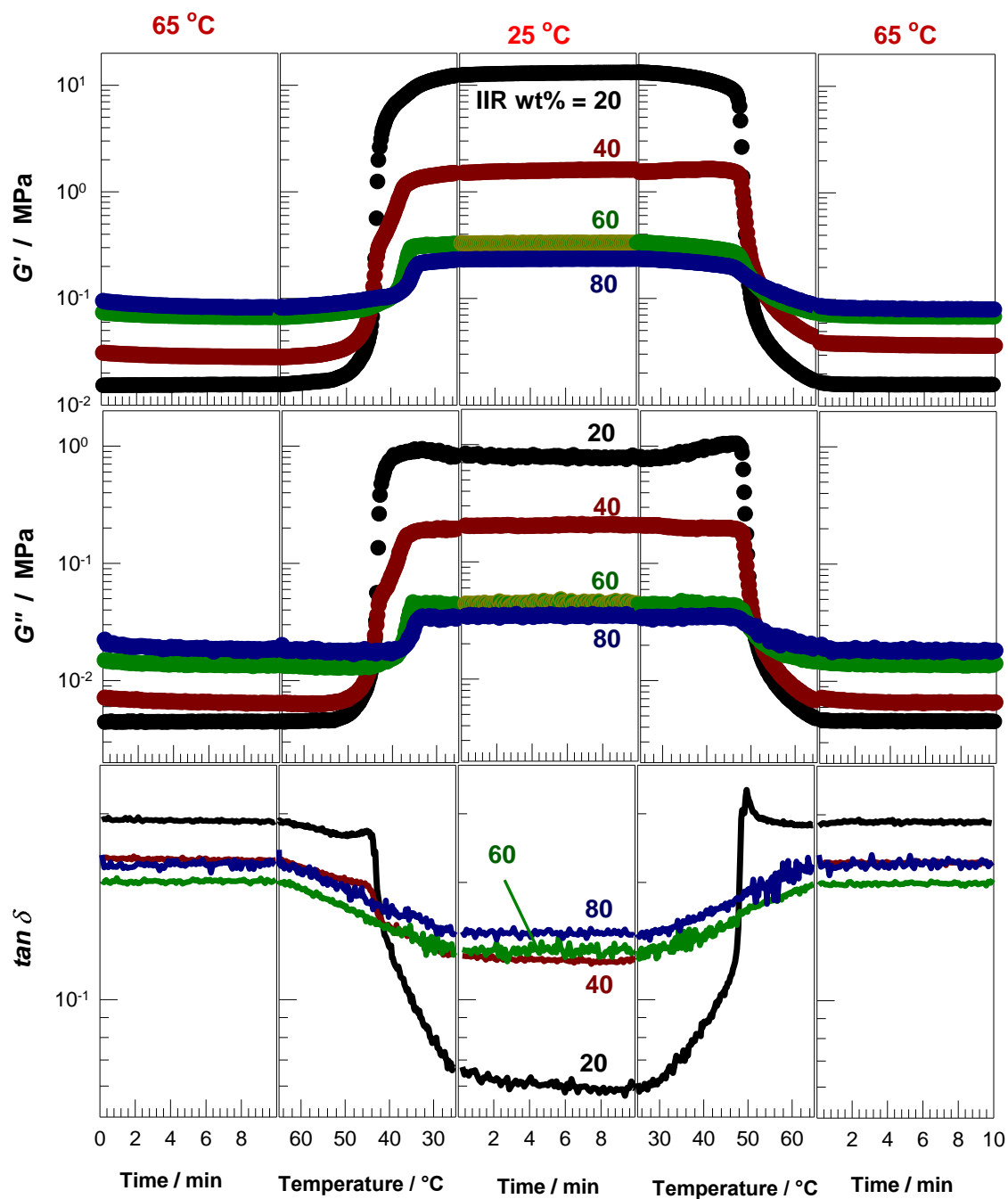
Fig. S4. *G'*, *G''*, and *tan δ* of IPNs during a cooling-healing cycle between 65 and 25 °C. IIR contents are indicated.

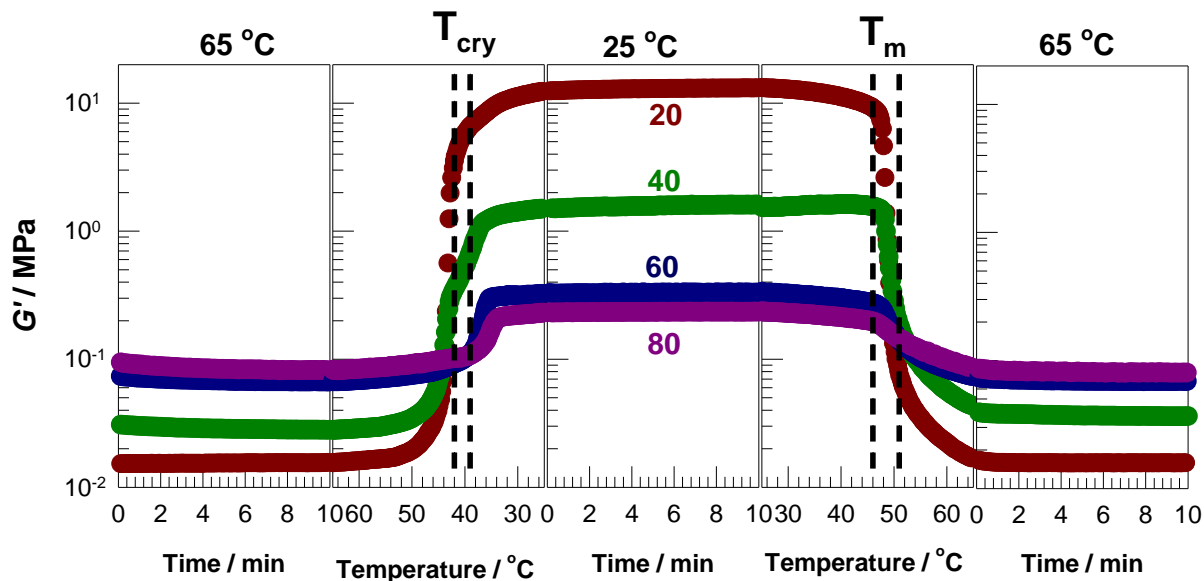**Fig. S5.** G' of IPNs during a cooling-healing cycle between 65 and 25 °C. The range of T_m and T_{cry} of IPNs is shown by the vertical dashed lines. IIR contents are indicated.
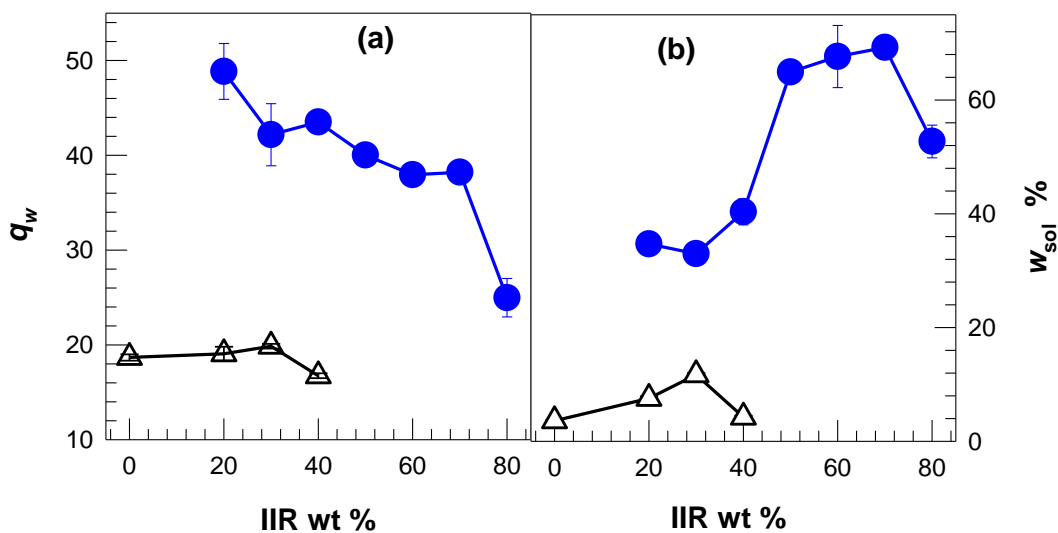

Fig. S6. The equilibrium weight swelling ratio q_w in toluene (left), and the soluble fraction w_{sol} of IPNs shown as a function of IIR wt%. The filled and open symbols represent the data of IPNs prepared with and without toluene, respectively.
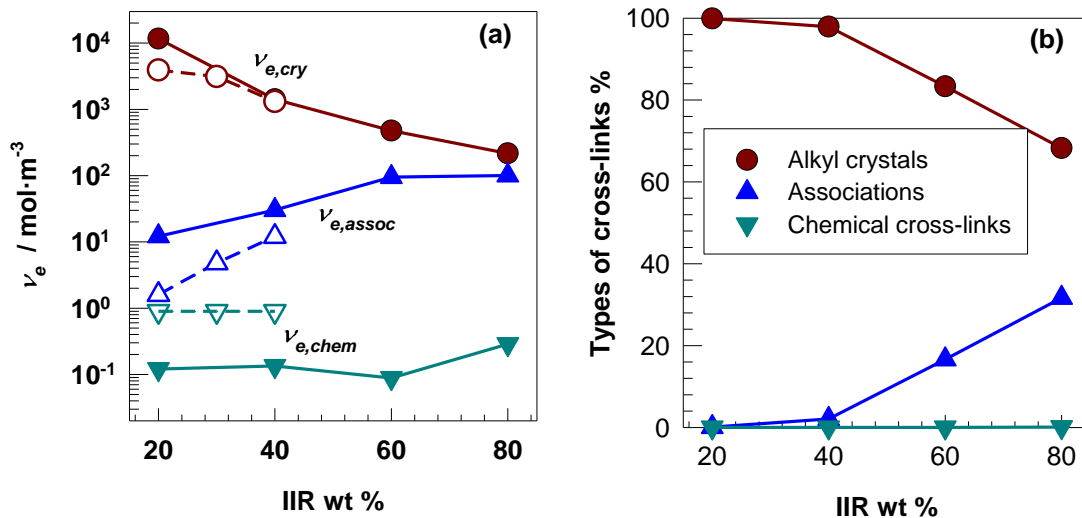
Fig. S7. (a) The cross-link density ν_e of IPNs due to the alkyl crystals $\nu_{e,cry}$, hydrophobic associations $\nu_{e,assoc}$, and chemical cross-links $\nu_{e,chem}$ plotted against their IIR contents. The open symbols show the data for IPNs prepared by bulk polymerization. **(b):** Contributions of these three types of cross-links to the total cross-link density of IPNs shown as a function of IIR wt%.
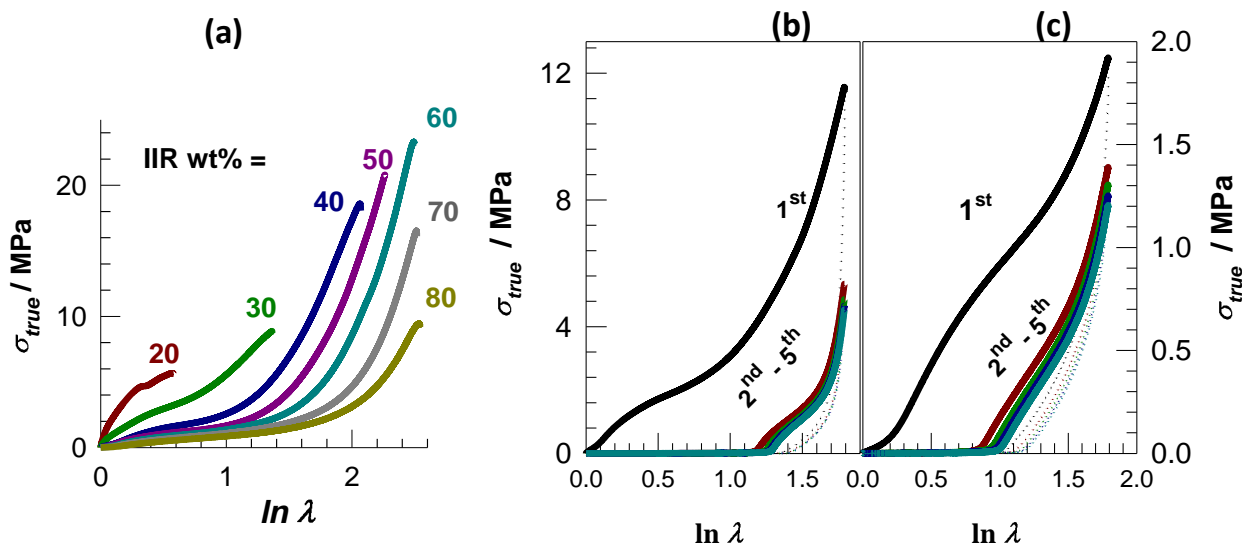

Fig. S8. Stress-strain curves and tensile cycles of IPNs given in Fig. 7a, 8a, b in the text replotted as the dependence of the true stress σ_{true} on true strain $ln\ \lambda$, where λ is the deformation ratio. Note that $\lambda = 1 + \varepsilon$, and $\sigma_{true} = \lambda\sigma_{nom}$.

References

[S1] S. R. Kline, J. Appl. Cryst. Reduction and Analysis of SANS and USANS Data Using IGOR Pro" 39 (2006) 895–900

[S2] D. I. Svergun, Restoring low resolution structure of biological macromolecules from solution scattering using simulated annealing. Biophys J.76 (1999) 2879–2886. pmid:10354416

[S3] L. A. Feigin, D. I. Svergun, Structure Analysis by Small-Angle X-Ray and Neutron Scattering, Plenum Press, New York (1987)

[S4] P. B. Moore, Small-angle scattering. Information content and error analysis, J. Appl. Cryst. 13, (1980) 168-175.

[S5] J. E. Mark, B. Erman, Rubberlike Elasticity; Cambridge University Press: Cambridge, U.K., 2007.

[S6] P. J. Flory, Principles of Polymer Chemistry; Cornell University Press: Ithaca, NY, 1953.

[S7] L. R. G. Treloar, The Physics of Rubber Elasticity; University Press: Oxford, 1975.

[S8] A. Matsuda, J. Sato, H. Yasunaga, Y. Osada, Order-disorder transition of a hydrogel containing an n-alkyl acrylate. Macromolecules 27 (1994) 7695−7698.

[S9] Y. Osada, A. Matsuda, Shape Memory in Hydrogels. Nature 376 (1995), 219.

[S10] C. Bilici, V. Can, U. Nöchel, M. Behl, A. Lendlein, O. Okay, Melt-processable shape-memory hydrogels with self-healing ability of high mechanical strength. Macromolecules 49 (2016) 7442−7449.

[S11] Y. Yang, C. Wang, C. G. Wiener, J. Hao, S. Shatas, R. Weiss, B. D. Vogt, Tough stretchable physically-cross-linked electrospun hydrogel fiber mats. ACS Appl. Mater. Interfaces 8 (2016) 22774−22779.

[S12 S. Durmaz, S. Fank, O. Okay, Swelling and mechanical properties of solution crosslinked poly(isobutylene) gels. Macromol. Chem. Phys. 203 (2002) 663−672.